Seamless fill of deep trenches by chemical vapor deposition: Use of a molecular growth inhibitor to eliminate pinch-off

Tushar K. Talukdar,[1,2] Gregory S. Girolami,[3] and John R. Abelson[1,a)]
[1]*Department of Materials Science and Engineering, University of Illinois at Urbana-Champaign, 1304 W. Green St, Urbana, Illinois 61801*
[2]*Department of Mechanical Science and Engineering, University of Illinois at Urbana-Champaign, 1206 W. Green St, Urbana, Illinois 61801*
[3]*School of Chemical Sciences, University of Illinois at Urbana-Champaign, 600 South Mathews Avenue, Urbana, Illinois 61801*

(Received 17 October 2018; accepted 7 January 2019; published 25 January 2019; corrected 30 January 2019)

Attempts to fill deep trenches by chemical vapor deposition often result in a "bread-loaf" profile, an overhang near the trench opening that arises whenever the growth rate is slightly higher near the opening than deeper in the feature. Continued growth leads to premature pinch-off at the opening, which leaves an undesirable void or seam along the centerline. Bread-loaf profiles can form even under superconformal growth conditions, as the authors recently found for the growth of HfO_2 from the precursor tetrakis(dimethylamino)hafnium and a forward-directed flux of H_2O coreactant. The current paper describes a method that can reduce or eliminate the bread-loaf problem: addition of an isotropic flow of a reactant that inhibits growth near the trench opening but leaves the growth rate unchanged deeper in the trench. A Markov chain model for ballistic transport of the inhibitor inside trenches is developed to account for this behavior: the model reveals that suppression of a bread-loaf profile is best accomplished with growth inhibitors that have a high sticking probability (>0.1 per wall collision) and that are consumed during growth. Four molecules are investigated as potential inhibitors during HfO_2 growth: tris(dimethylamino)silane, 3DMAS; methoxytrimethylsilane, MOTMS; hexafluoroacetylacetone, H(hfac); and acetylacetone, H(acac). The molecules 3DMAS and MOTMS inhibit growth but do so everywhere. As a result, they improve conformality, but are unable to eliminate the bread-loaf profile. In contrast, relatively small partial pressures (fluxes) of H(hfac) or H(acac) strongly inhibit HfO_2 growth and do so selectively on the upper substrate surface and near trench openings. In conjunction with the use of a forward-directed water flux that affords superconformal growth, the use of H(hfac) or H(acac) enables seamless fill of HfO_2 in trenches with aspect ratios as large as 10. *Published by the AVS.* https://doi.org/10.1116/1.5068684

I. INTRODUCTION

Complete filling of deep trenches or vias, without leaving a void or seam inside, is a key process step in the fabrication of advanced microelectronic and photonic devices.[1–5] As device sizes shrink, the effective aspect ratio (AR) of these structures increases,[6] which makes seamless filling more difficult to achieve: either the film growth kinetics must be made superconformal (i.e., faster at greater depths) or the feature must have sloped walls such that the initial trench geometry is wider near the opening than at the bottom.[7–9] A related problem in filling of deep structures is the formation of an overhang near the opening, called a "bread-loaf" coating profile.[10] The bread-loaf effect, which is due to fast growth outside of and near the trench opening, eventually leads to pinching-off of the opening before filling is complete and formation of a void or seam along the trench centerline. Chemical vapor deposition (CVD) with periodic plasma etch-back can prevent bread-loaf formation,[10] but the plasma often causes damage that unacceptably degrades device performance.[11–13]

Here, we present an alternative method to avoid bread-loaf profiles, in which a growth inhibitor of a carefully chosen type is added continuously during the CVD process. We previously reported three examples of growth inhibitors which are *nonconsumable* [Fig. 1(a)], meaning that they adsorb reversibly on the growth surface and reduce the film growth rate, but ultimately desorb intact: the use of NH_3 during HfB_2 growth from $Hf(BH_4)_4$ (the film composition contains <5 at. % N),[14] the use of 1,2-dimethoxyethane (dme) during TiB_2 growth from $Ti(BH_4)_3(dme)$,[15] and the use of vinyltrimethylsilane (VTMS) during Cu growth from Cu(hfac) VTMS.[16] In the first of these cases, inhibition is due to site blocking by NH_3. In the latter cases, the inhibitor appears to stimulate the associative desorption of the precursor fragment, $Ti(BH_4)_3$ or Cu(hfac), respectively, from the growth surface; site blocking may occur, but is not required to explain the reduced growth rate. Note that because the initial precursor adsorption step releases dme or VTMS, respectively, the net reaction conserves inhibitor molecules, i.e., they are nonconsumable.

Due to the reversibility, a nonconsumable inhibitor will reach an equilibrium partial pressure everywhere inside the feature and thus reduce the growth rate on all the surfaces. The net effect is that nonconsumable inhibitors enhance conformality—and thus are very important for situations in which the desired product is coating rather than

a)Electronic mail: abelson@illinois.edu

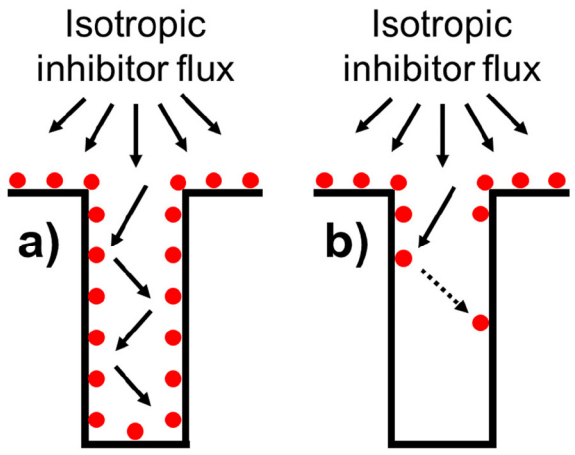

FIG. 1. Schematic diagram of the steady-state distribution of inhibitor molecules inside narrow trenches. (a) Nonconsumable inhibitor in adsorption equilibrium affords the same inhibition on all surfaces; (b) consumable inhibitor with high sticking probability affords inhibition only on upper surfaces. In both cases, the inhibitor has an isotropic (uniform) flux distribution outside the trench.

complete filling—but they do not differentially eliminate the bread-loaf problem.

Here, we demonstrate a solution to the bread-loaf problem using growth inhibitors that are *consumable* [Fig. 1(b)], meaning that they can adsorb irreversibly on the growth surface. The adsorbed intermediates generated by the inhibitor either become incorporated into the film, or they convert into new species that desorb. As we will show below, to eliminate bread-loaf formation, the consumable inhibitor should have two properties: (1) it reduces the film growth rate owing to passivation of surface sites by reaction with (or site blocking by) the adsorbed inhibitor or its intermediates, and (2) any desorbing species formed from the inhibitor are unable to serve as growth inhibitors. These features assure that inhibition takes place selectively near the trench opening, because the inhibitor reacts there before it can diffuse deeply into the feature.

We previously reported several examples of consumable inhibitors in CVD processes (Table I). For growth of CrB_2 from the precursor $Cr(B_3H_8)_2$, we showed that H atoms generated from a remote H_2 plasma source reduce the CrB_2 growth rates at the trench opening by >50%; the result is that film thickness increases with depth (it is superconformal).[17] In this system, the plasma-generated H atoms ultimately desorb from the surface as H_2 and are not incorporated into the film. For HfB_2 film growth from $Hf(BH_4)_4$, we found that addition of N atoms and hexafluoroacetylacetone [H(hfac)] to the growth flux decrease the growth rate by >80%, and addition of $Pd(hfac)_2$ completely suppresses film growth.[17] In these cases, heteroatoms from these inhibitors become incorporated into the film and change its composition.

In the current work, we apply these ideas to our recently described demonstration of the superconformal CVD of HfO_2 from tetrakis(dimethylamino)hafnium (TDMA-Hf) and a forward-directed flux of H_2O.[8] The forward-directed flux scatters when it reaches the bottom of a trench, thus creating a virtual source of water. Because the scattered flux of water is greatest at the trench bottom, the growth rate within the trench is fastest there. However, the total flux of water (isotropic plus forward-directed) is even larger on the substrate surface; consequently, the rapid growth of oxide outside the trench eventually forms a bread-loaf profile at the trench opening that pinches-off before complete fill. The time evolution of the bread-loaf shape and the ultimate failure due to pinch-off in a trench with an aspect ratio of 3 is depicted in Figs. 2(a)–2(c). Here, we explore whether the bread-loaf effect in this HfO_2 system can be avoided by adding a growth inhibitor (Table I). We find that two such inhibitors, H(hfac) and acetylacetone [H(acac)], can prevent bread-loaf formation and pinch-off at the trench opening and enable complete seamless fill in trenches with aspect ratios up to 10. We use a Markov chain model for ballistic transport-reaction within the trench to calculate the inhibitor flux (and consumption rate) for different values of the inhibitor sticking probability; the simulation results provide upper and lower bounds on the reaction kinetics that an inhibitor should exhibit for best results.

TABLE I. List of inhibitors explored by our group based on their sticking probability and incorporation into the film.

Inhibitor	Film material	Inhibitor sticking probability	Inhibitor incorporation	Heteroatom (impurity)	Reference
H-atom	CrB_2	High	Low[a]	None	17
N-atom	HfB_2	High	High	N	17
H(hfac)	HfB_2	High	High	C, F	17
Pd(hfac)	HfB_2	Very high (renucleates)	High	Pd, C, F	17
3DMAS	HfO_2	Low[b]	Low	None	This work
MOTMS	HfO_2	Low[b]	Low	C, Si	This work
H(hfac)	HfO_2	High	High	C, F	This work
H(acac)	HfO_2	High	High	C	This work

[a]H atoms are removed from the growth surface by recombinative desorption.
[b]For the case of nonconsumable inhibitors (i.e., reversible adsorption), this table entry refers to the net adsorption constant.

II. EXPERIMENT

The film growth experiments are conducted in a turbopumped cold-wall CVD system with a base pressure of 5×10^{-8} Torr, most of which is H_2. The substrate is radiatively heated to 200 °C by a tungsten wire mounted behind the substrate holder; the temperature is measured by a K-type thermocouple probe clamped to a spot on the substrate holder plate. The TDMA-Hf precursor (≥99.99%) and inhibitors [tris(dimethylamino)silane (3DMAS), methoxytrimethylsilane (MOTMS), H(hfac), and H(acac)] are obtained from Sigma-Aldrich and kept in Pyrex containers equipped with stainless-steel fittings. Flow regulation of TDMA-Hf is controlled by heating the source container to temperatures of 25–50 °C; the delivery tube is heated to 80 °C (slightly below the precursor decomposition temperature of 90 °C) to avoid condensation on its walls; no carrier gas is used for the precursor. For all four inhibitors, flow is controlled with needle valves. Deionized (DI) water at room temperature is

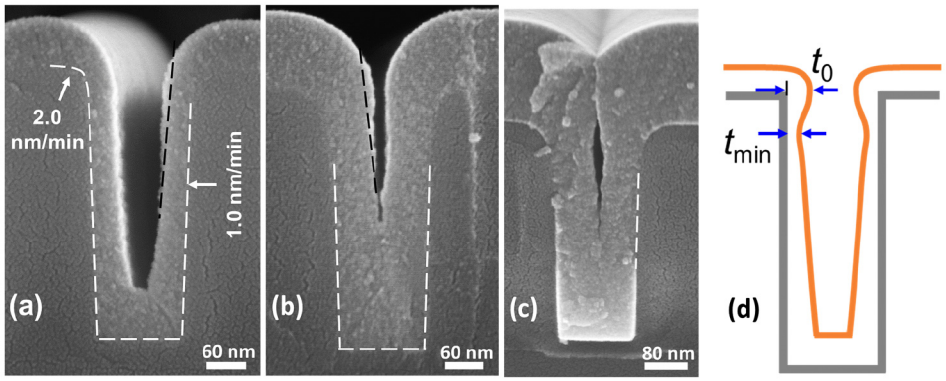

FIG. 2. (a)–(c) Cross-sectional SEM image of trenches with an aspect ratio of 3, coated with 0.18 mTorr TDMA-Hf and 0.023 mTorr H_2O at 200 °C for (a) 40 min, (b) 60 min, and (c) 90 min. A black dashed line is added in (a) and (b) to highlight the bread-loaf shape at the trench opening. (d) Schematic of a coating profile inside a rectangular trench describing the bread-loaf ratio, t_0/t_{min}, at the trench opening.

used as the coreactant; the water partial pressure is also controlled with a needle valve.

Precursor, water, and inhibitor are supplied to the growth chamber through separate stainless-steel tubes (4 mm i.d.). The precursor and water delivery tubes can be pointed directly normal to the substrate (they terminate 7 cm away from the substrate surface) or at the chamber sidewall. The water delivery tube is pointed at the substrate (forward-directed) unless otherwise stated. The inhibitor tube is always pointed at the reactor wall to obtain an isotropic flux distribution over the substrate surface. A TDMA-Hf pressure of 0.09–0.18 mTorr and an H_2O pressure of 0.009–0.023 mTorr are used in this work; these pressure ranges provide superconformal HfO_2 coatings in trenches.[8] The inhibitor pressure is varied within a range of 0.01–2.60 mTorr. The partial pressures reported here are the average values inside the reactor, which were measured with only precursor or only water or only inhibitor flowing before the growth experiments. The forward-directed fluxes on the growth surface are higher than those given by the isotropic pressures. During film deposition, a slow rate of reaction in the gas phase or on the room-temperature chamber walls may consume a portion of the molecules; hence, the partial pressures above the substrate during growth may be smaller than those measured above.

Growth rate measurements are done on 1.5 × 1.0 cm planar Si and 300 nm thermal SiO_2/Si wafers. The Si wafers are cleaned with standard solvents (in the order of acetone, isopropyl alcohol, DI water, and isopropyl alcohol) and then dried in an N_2 flow; this protocol does not etch the native oxide. For conformal coating and filling studies, lithographically defined microtrenches with SiN walls are used. The SiN microtrench substrates include variable aspect ratio trenches (range 1–20) on the same sample, which allows us to determine in a single experiment the upper limit of trench aspect ratio that can be filled using the given growth conditions.

Film microstructure and thickness are determined by cross-sectional scanning electron microscopy (SEM). The refractive indices of HfO_2 films are derived from *ex situ* variable angle spectroscopic ellipsometry (SE) data acquired at incident angles of 50°, 60°, and 70° and fit to the Cauchy equation; the refractive index of the CVD HfO_2 film was previsouly found to be lower than bulk HfO_2 by about 10%.[8] The film thickness during growth is determined from *in situ* SE data using the derived indices and a multilayer optical model, consisting of the Si substrate, native oxide on Si, and the deposited HfO_2 film; surface and interfacial roughness layers are not included because the silicon and oxide surfaces are very smooth as observed in SEM. The film thickness measured by ellipsometry is within ±5% of that determined from SEM cross-sectional images. The reported film growth rate is the final thickness divided by the duration of growth; this calculation assumes the absence of a significant nucleation delay, which we verified by real-time SE in the growth chamber. Rutherford backscattering spectrometry (RBS) is used to measure the areal density of Hf atoms; the resulting value is divided by the film thickness as measured by SEM to give the density of the Hf sublattice. Auger electron spectroscopy (AES) is used to identify the chemical elements in the film, but the AES results are at best only semiquantitative owing to charging of the HfO_2 film surface and the preferential erosion of lighter elements. For these reasons, the chemical compositions we report are determined by x-ray photoelectron spectroscopy (XPS).

III. RESULTS AND DISCUSSION

A. Preliminary assessment of possible growth inhibitors

The goal of the current experiments is to determine whether a growth inhibitor can eliminate the bread-loaf effect —the formation of an overhang near trench openings—that is often seen in efforts to fill deep features by chemical vapor deposition. The system we have chosen to study is one we have recently reported: the deposition of HfO_2 from TDMA-Hf and a forward-directed flux of H_2O.[8] This process works extremely well in deep features to afford films that are superconformal (the growth rate increases with depth), except that it suffers from the formation of a bread-loaf profile near the trench opening.

Our approach is to seek inhibitors that prevent the formation of a bread-loaf profile. As mentioned in the introduction,

this outcome will require a consumable inhibitor with a medium to high sticking probability; these attributes will prevent the inhibitor from diffusing deeply into the feature, so that the inhibition effect will be confined to the surface and near-surface regions of the trenches. Toward this end, we have investigated four possible growth inhibitors: 3DMAS, MOTMS, H(hfac), and H(acac).

The magnitude of the effect we are seeking can be defined as follows. The geometry of a bread-loaf shape can be described by the ratio of maximum film thickness at the trench opening (t_0) to that at just below the opening where the bread-loaf shape has minimum thickness (t_{min}) [Fig. 2(d)]; we refer to the quotient t_0/t_{min} as the "bread-loaf ratio." To avoid pinch-off at the trench opening, the bread-loaf ratio must be 1 (or less), *which is a key criterion for complete fill*. The trench in Fig. 2(a) has a bread-loaf ratio of ~2; a similar value results for the other HfO_2 film growth conditions used in the present experiments and in our previous report.[8] To reduce the bread-loaf ratio to ≤1, a successful inhibitor for complete fill should therefore reduce the growth rate at the trench opening by at least 50%.

1. Tris(dimethylamino)silane (3DMAS), $[(CH_3)_2N)]_3SiH$

The aminosilane 3DMAS is commonly used as an atomic layer deposition (ALD) precursor for SiO_2 growth; the onset temperature for reaction with H_2O is about 400 °C.[18] We first carried out a control experiment to verify that SiO_2 is not deposited from 3DMAS at the lower temperatures (200 °C) characteristic of our HfO_2 experiments. Thus, a planar Si substrate at 300 °C and an SiO_2 substrate at 280 °C were exposed to 0.25 mTorr 3DMAS and 0.5 mTorr H_2O. For both substrates, the 3DMAS partial pressure was increased to 2.3 mTorr after 10 min. The *in situ* SE data show no change with time for either substrate, i.e., no SiO_2 nucleation and growth occurs from 3DMAS and H_2O at $T \leq 300$ °C (supplementary material).[25]

With this result in hand, we then turned to the question whether addition of a coflow of 3DMAS inhibits HfO_2 growth on a planar substrate at 200 °C. For growth from 0.18 mTorr TDMA-Hf and 0.019 mTorr H_2O [Fig. 3(a)], we find that added 3DMAS does decrease the growth rate, but the effect is modest: for a 3DMAS pressure of 0.25 mTorr, the decrease in the growth rate is ~24%, and at 2.1 mTorr, the decrease is ~47%. In the latter case, some of the decrease in the growth rate may be due to increased gas-phase scattering of the forward-directed water coreactant before it reaches the surface.[19]

The inhibition effect on HfO_2 growth was then examined in a trench with an aspect ratio of 6. In the absence of the inhibitor, using 0.18 mTorr TDMA-Hf and 0.023 mTorr H_2O at 200 °C, the growth rate is 2.0 nm/min at the top surface and 1.0 nm/min on the sidewall at mid-depth, and within the trench, the thickness is nearly uniform [Fig. 4(a)]. When 3DMAS is coflowed at a pressure of 0.25 mTorr, the growth rate is 1.4 nm/min at the top surface and 0.7 nm/min on the sidewall at mid-depth [Fig. 4(b)]. The percentage decrease in the growth rate on all surfaces is essentially the same as

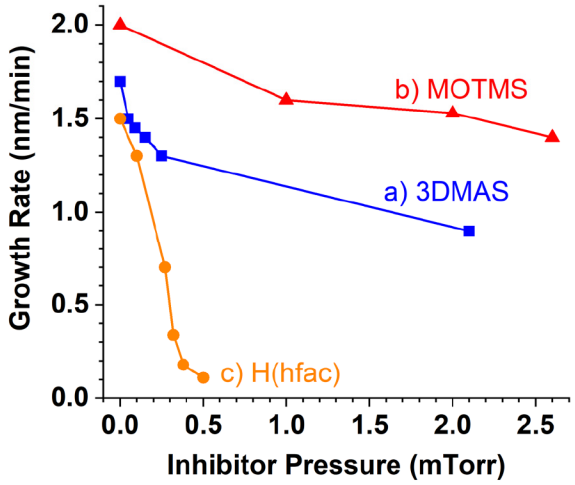

FIG. 3. HfO_2 growth rates on planar Si (100) substrates at 200 °C measured by spectroscopic ellipsometry as a function of the inhibitor partial pressure. (a) 3DMAS inhibitor coflowed with 0.18 mTorr TDMA-Hf and 0.019 mTorr H_2O. (b) MOTMS inhibitor coflowed with 0.18 mTorr TDMA-Hf and 0.023 mTorr H_2O. (c) H(hfac) inhibitor coflowed with 0.09 mTorr TDMA-Hf and 0.014 mTorr H_2O. Lines through data points are guides for the eye only.

observed on the planar substrate, and the bread-loaf ratio remains unchanged at 2. (Note that if the deposit without the inhibitor had been subconformal, then the use of the inhibitor would have rendered it more conformal due to the reduced rate of gas depletion down the axis of the trench. But since the starting state is essentially conformal, that effect is not seen.)

The refractive index of HfO_2 grown with or without 3DMAS is essentially identical (Fig. 5), which suggests that the incorporation of C, N, or Si atoms into the film, caused by the coflow of 3DMAS, is low. This conclusion is verified by the XPS composition shown in Table II; the elemental atomic concentrations for a film grown with 0.25 mTorr 3DMAS coflow is similar to another film grown without

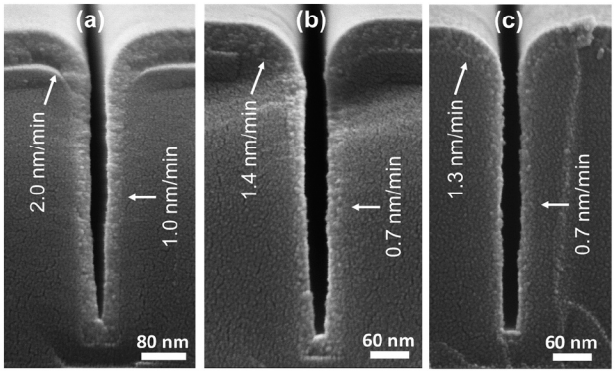

FIG. 4. Cross-sectional SEM images of trenches coated using 0.18 mTorr HfO_2 and 0.023 mTorr H_2O at 200 °C for 30 min. (a) Without inhibitor (AR = 6). (b) With 0.25 mTorr 3DMAS (AR = 6). (c) With 2.6 mTorr MOTMS (AR = 7). In both Figs. 5(b) and 5(c), the growth rate is reduced by ~30% both at the top surface and at sidewall near the middle of the trenches; however, the bread-loaf ratio (~2) is unaffected by these inhibitors in the present experiments.

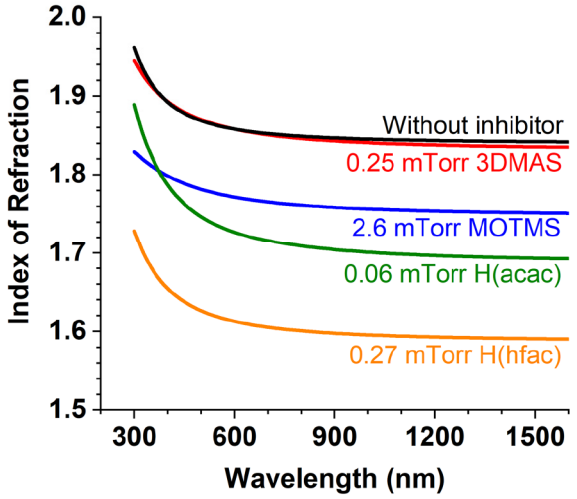

FIG. 5. Refractive index of an HfO_2 film grown without any inhibitor or with coflow of different inhibitor molecules.

inhibitor coflow. This finding and the uniform decrease in the film growth rate are characteristics of a nonconsumable inhibitor. Although 3DMAS is unable to suppress bread-loaf formation, it could be useful in enhancing the conformality of HfO_2 growth in high aspect ratio trenches.

2. Methoxytrimethylsilane (MOTMS), $CH_3OSi(CH_3)_3$

In the sol–gel literature, MOTMS is reported to react with silica to convert surface –OH (hydroxyl) groups to $-OSi(CH_3)_3$ (trimethylsiloxyl) groups;[20] this reactivity motivated us to test MOTMS as an HfO_2 growth inhibitor. The results are similar to those seen for 3DMAS: when a planar substrate is exposed to 0.18 mTorr TDMA-Hf, 0.023 mTorr H_2O at 200 °C, addition of 2.6 mTorr of MOTMS decreases the HfO_2 growth rate by ~30% [Fig. 3(b)]. In a trench with an aspect ratio of 7, the film growth rate is slightly reduced [Fig. 4(c)], but the bread-loaf ratio remains unchanged (~2), as seen for 3DMAS [Fig. 4(b)]. Thus, MOTMS behaves like a nonconsumable inhibitor that is unable to correct the bread-loaf profile for the present HfO_2 deposition process. Films grown in the presence of MOTMS have a slightly lower refractive index than those grown in the absence of MOTMS (Fig. 5). RBS suggests that this difference is due to a reduced film density: the density for the Hf sublattice decreases from 86% of bulk (when no inhibitor is present) to 77% of bulk (in the presence of MOTMS). XPS data show that 2.6 mTorr MOTMS coflow has little effect on the film composition: it leads to the incorporation of ~1 at. % of silicon, an increase in the carbon content by ~2 at. %, and leaves the concentrations of other elements (Hf, O, and N) unchanged (Table II).

TABLE II. Growth conditions and XPS atomic concentrations (at. %) for selected films grown from TDMA-Hf precursor and H_2O at 200 °C. XPS composition is calculated from high resolution peaks obtained after 2 min of argon sputtering to remove surface carbon contamination.

Inhibitor	$P_{precursor}$ (mTorr)	P_{H_2O} (mTorr)	Atomic concentration (at. %) Hf	O	C	N	F	Si
None	0.09	0.014	32	62	3.0	3.0	—	—
0.25 mTorr 3DMAS	0.18	0.023	32	62	3.0	3.0	—	—
2.6 mTorr MOTMS	0.18	0.023	31	60	5.0	3.0	—	1.0
0.1 mTorr H(hfac)	0.09	0.014	26	45	12	6.0	11	—
0.27 mTorr H(hfac)	0.09	0.014	25	43	11	6.0	15	—
0.06 mTorr H(acac)	0.09	0.014	28	53	15	4.0	—	—
0.09 mTorr H(acac)	0.09	0.014	27	52	17	4.0	—	—
0.12 mTorr H(acac)	0.09	0.014	27	51	17	5.0	—	—

3. Hexafluoroacetylacetone [H(hfac)], $CF_3COCH_2COCF_3$

We previously reported that H(hfac) strongly inhibits the growth of HfB_2 from the single-source precursor, $Hf(BH_4)_4$.[17] Of relevance in the current context is that H(hfac) is an acid that can etch metal oxides to afford metal chelates and water as by-products.[21] We expect that the etch rate of HfO_2 will be small under our growth conditions, but we verified this expectation with a control experiment in which we used SE to monitor the thickness of a preformed HfO_2 film upon exposure to H(hfac) at 200 °C. We find that the observed HfO_2 etch rates are 0.005 and 0.017 nm/min at H(hfac) pressures of 3 and 40 mTorr, respectively (Fig. 6). As we will see below, these etch rates are negligibly small.

With this control experiment in hand, we then studied the effect of coflow of H(hfac) on HfO_2 deposition onto planar substrates from 0.09 mTorr TDMA-Hf and 0.014 mTorr H_2O at 200 °C. We find that the growth rate is reduced by 77% at an H(hfac) pressure of 0.32 mTorr and by over 90% at 0.5 mTorr [Fig. 3(c)]. As judged from these results, we would expect that an H(hfac) pressure of just under 0.32 mTorr should reduce the growth rate by 50%, which is the amount we seek (see above). Such pressures should therefore have a significant effect on the bread-loaf effect for deposition of HfO_2. For these experiments, we employed

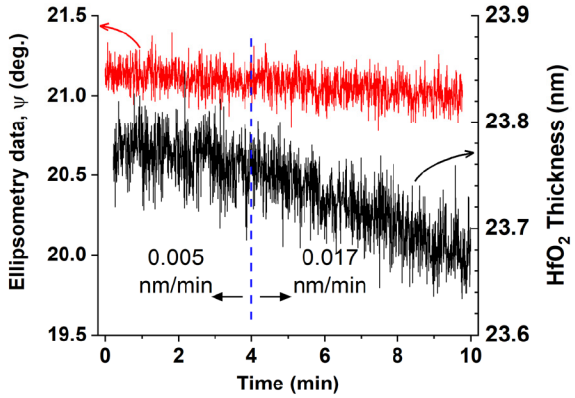

FIG. 6. Ellipsometry data for possible etching of an HfO_2 film deposited with 0.09 mTorr TDMA-Hf and 0.014 mTorr H_2O at 200 °C: *in situ* SE data (red curve) and the corresponding HfO_2 thickness (black curve) at 200 °C with an H(hfac) flow of 3 mTorr for the first 4 min (etch rate = 0.005 nm/min) and 40 mTorr for the next 6 min (etch rate = 0.017 nm/min).

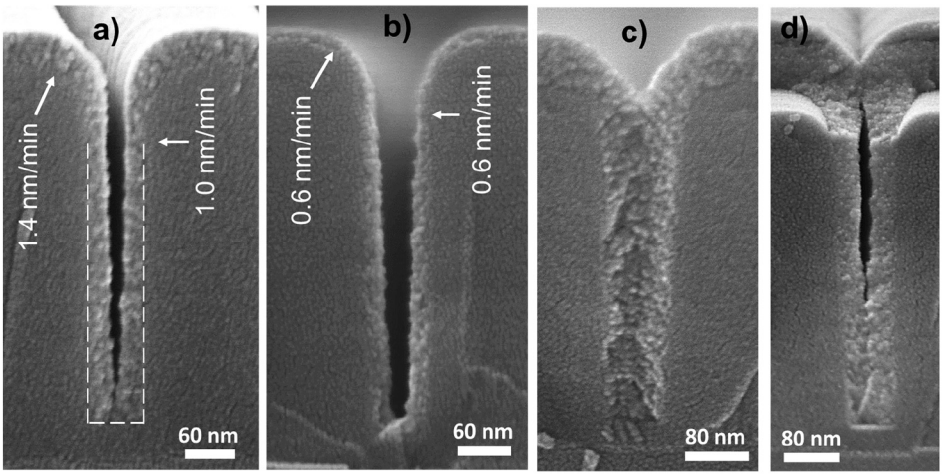

FIG. 7. Cross-sectional SEM images of trenches, coated with 0.09 mTorr TDMA-Hf, 0.014 mTorr H_2O, and variable H(hfac) pressure at 200 °C. (a) 0.1 mTorr H(hfac) for 30 min (AR = 7); the bread-loaf ratio is ~1.4. (b) 0.27 mTorr H(hfac) for 30 min (AR = 6); the bread-loaf ratio is ~1. (c) Complete fill in a trench: same conditions as in (b) for 60 min. (d) Void formation: conditions as in (c) but without coflowing H(hfac).

trenches with aspect ratios of 6–7 and kept the temperature and the TDMA-Hf and H_2O pressures the same as those above.

At a coflow of 0.1 mTorr H(hfac), the resulting profile has a bread-loaf ratio of 1.4 [Fig. 7(a)]; this ratio is 30% smaller than that seen (as described above) in the absence of H(hfac). Remarkably, at an H(hfac) pressure of 0.27 mTorr, the bread-loaf ratio is ~1 (i.e., reduced by 50% from the value in the absence of the inhibitor), which is ideal for filling [Fig. 7(b)]. Moreover, the gradual increase in the film growth rate on the lower sidewalls of the trench [Fig. 4(a)] is preserved. If deposition is continued under these conditions for longer times, complete seam-free filling of the trench results [Fig. 7(c)]. For comparison, under identical growth conditions but without any inhibitor, a trench of the same aspect ratio pinches-off and leaves a large void [Fig. 7(d)].

For films grown under these circumstances (i.e., 0.09 mTorr TDMA-Hf and 0.014 mTorr H_2O at 200 °C), the refractive index of HfO_2 decreases by ~13% when 0.27 mTorr H(hfac) is added, versus when it is absent (Fig. 5). The reduction in the refractive index can be ascribed to a decrease in the film density from 86% of the bulk value (for films deposited in the absence of the inhibitor) to ~68% for those deposited in the presence of H(hfac), as shown by RBS. Some of the decrease may also be due to the incorporation of some hfac heteroatoms (F and C) into the film, as verified by XPS (Table II) and an AES depth profile (supplementary material).[25]

4. Acetylacetone [H(acac)], $CH_3COCH_2COCH_3$

H(acac) is a halogen-free analog of H(hfac); it is a weaker acid and is less likely than H(hfac) to serve as an oxide etchant. It has recently been reported that it can serve as an inhibitor for area selective ALD of SiO_2 on dielectric surfaces.[22]

We find that, for growth of HfO_2 onto planar substrates from 0.09 mTorr TDMA-Hf and 0.014 mTorr H_2O at 200 °C, adding H(acac) pressures up to 0.05 mTorr *increases* the growth rate by up to a factor of 2 (Fig. 8); this behavior is not understood at present. At H(acac) pressures of 0.05 mTorr and above, however, H(acac) increasingly inhibits HfO_2 growth. For a film grown on a planar Si substrate from 0.09 mTorr TDMA-Hf, 0.014 mTorr H_2O, and 0.06 mTorr H(acac) at 200 °C, the growth rate is reduced by about 50% versus the rate in the absence of H(acac). For the resulting film, the refractive index at 600 nm is smaller by ~7% versus the index for a film grown in the absence of the inhibitor (Fig. 5); this decrease can be attributed to a decrease in the film density from 86% of the bulk value (for films deposited in the absence of the inhibitor) to ~73%. The H(acac) also leads to the incorporation of ~12% of carbon in the film (Table II); the presence of carbon is also verified by TEM (see below).

In Secs. III B–III D, we describe additional experiments with H(acac) as an inhibitor for HfO_2 growth. For the purpose of the present study (to suppress the formation of a

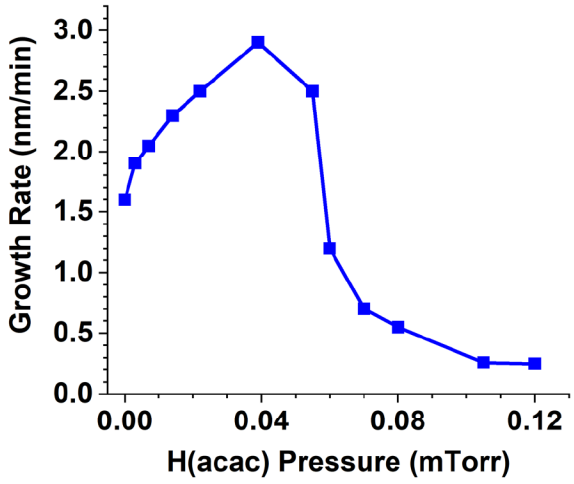

FIG. 8. Film growth rates on a planar Si substrate as a function of H(acac) pressure that is coflowed with 0.09 mTorr TDMA-Hf plus 0.014 mTorr H_2O at 200 °C. The line through the data points is a guide for the eye only.

bread-loaf at the trench opening), we focus only on the pressure range in which H(acac) causes inhibition.

B. Complete fill in trenches with nearly parallel sidewalls

We next investigated film growth in trenches with 0.09 mTorr TDMA-Hf and 0.014 mTorr H_2O at 200 °C, plus a coflow of H(acac). For an H(acac) pressure of 0.06 mTorr, complete fill in a trench with an aspect ratio of 5 is achieved over 60 min [Fig. 9(a)]. A slight increase of the H(acac) pressure to 0.07 mTorr affords complete fill in trenches with aspect ratios of up to 9 [Fig. 9(b)], and further increasing the H(acac) pressure to 0.09 mTorr significantly improves the fill in trenches with aspect ratios of up to 11.5 [Fig. 9(c)].

For the film shown in Fig. 9(b), grown in a trench with an aspect ratio of 7, the fill quality was examined by cross-sectional TEM. The bright field TEM image reveals a subtle low-density seam near the bottom of the trench, whereas the fill is dense and free of any seam in the top half of the trench [Fig. 10(a)]. We previously reported that—to convert a rectangular trench to a V-shaped one such that the V angle is higher than the critical value of 2°—the fraction of the forward-directed water flux must be above a certain value that depends on the aspect ratio.[8] In the present experimental setup, the fraction of the forward-directed water flux is about 40%. The presence of a subtle seam in Fig. 10(a) suggests that an increase in that fraction, which is possible in a reactor with a higher pumping rate, will be required to fill this trench completely without any seam.

The energy dispersive x-ray spectroscopy (EDS) element map obtained by TEM shows that a low concentration of N [Fig. 10(b)] and a moderate amount of C [Fig. 10(c)] are present in the HfO_2 film; this result is consistent with the composition deduced from XPS (Table II). A small decrease in the film refractive index is seen (Fig. 5) when H(acac) is present during growth. Note that the trench sidewall material is SiN_x, so a bright N signal is observed at the sidewalls. The brightness of the C signal in the fill inside the trench is less than

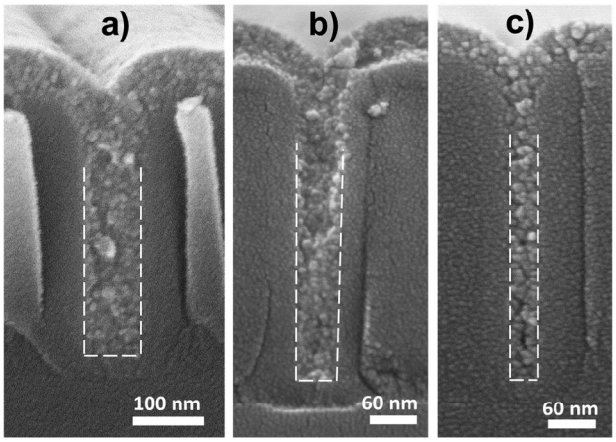

FIG. 9. Complete fill in trenches with different AR, coated using 0.09 mTorr TDMA-Hf, 0.014 mTorr H_2O, and variable H(acac) pressure at 200 °C. (a) 0.06 mTorr H(acac) for 60 min (AR = 5). (b) 0.07 mTorr H(acac) for 60 min (AR = 9). (c) 0.09 mTorr H(acac) for 75 min (AR = 11.5).

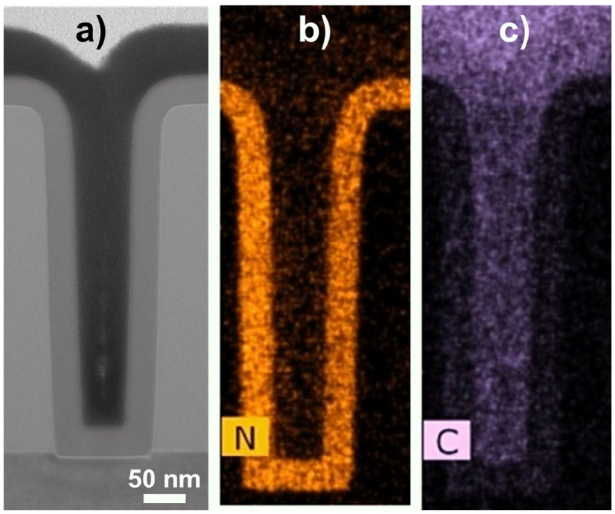

FIG. 10. (a) Bright field TEM image of a trench with AR = 7 from the same sample as in Fig. 9(b); there is a subtle low-density seam near the bottom of the trench. (b) and (c) TEM-EDS elemental maps of N (b) and C (c) for the same sample as in (a).

that in the film outside the trench; this finding is consistent with a large reduction in the inhibitor incorporation rate with depth when the inhibitor sticking probability is high (discussed in Sec. III E).

C. Effect of higher inhibitor pressures

To investigate if the fill can be improved in trenches with aspect ratios greater than 10, we employed higher inhibitor pressures. The idea is to reduce the film growth rate to a significant depth below the bread-loaf at the opening, thereby enhancing the V angle when the rectangular trench converts to a V-shaped trench. Interestingly, when the H(acac) pressure is increased to 0.12 mTorr, keeping the other conditions the same as in Fig. 9, the growth rate decreases similarly on all surfaces [Fig. 11(a)]: on the top surface the film growth rate is ~0.23 nm/min, consistent with Fig. 8, and the bread-loaf ratio reverts back to that obtained without coflowing any inhibitor [Fig. 4(a)]. A similar result is seen for a 0.32 mTorr H(hfac) pressure, with other conditions the same as in Fig. 11(a), in a trench with an aspect ratio of 8 [Fig. 11(b)]. In both these cases, we suggest that the inhibitor pressure is high enough to create a saturated surface coverage and thus a lower sticking rate, which leads to a nearly constant inhibitor pressure at all depths in the trench. Under these conditions, the inhibitor affords highly conformal films in recessed structures with very high aspect ratios.

D. Coating in trenches with a re-entrant geometry

In a re-entrant trench, the width is minimum at the opening and increases with depth [Fig. 12(a)]. Conformal coating in such a trench is extremely difficult because of the low conductance of the reactant molecules through the narrow opening, and complete fill is simply impossible even for a highly conformal process due to the pinch-off that will

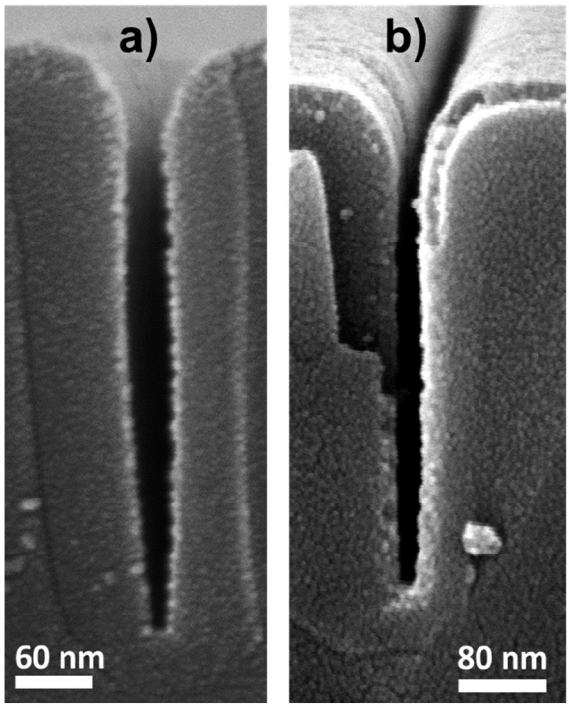

FIG. 11. Cross-sectional SEM image of trenches coated by coflowing inhibitors with 0.09 mTorr TDMA-Hf and 0.014 mTorr H_2O at 200 °C for 80 min: (a) 0.12 mTorr H(acac) in a trench with AR = 11.5 and (b) 0.32 mTorr H(hfac) in a trench with AR = 8.

necessarily occur at the narrow opening. To fill such a geometry requires either (i) a true bottom-up process that selectively grows the film only from the bottom surface, or (ii) a superconformal process with a step coverage large enough (i.e., much larger than 1) to compensate for the decreasing width from the top to the bottom.

In preliminary attempts to fill re-entrant trenches, we tested our superconformal process based on a forward-directed water flux, along with a coflow of H(acac) inhibitor to suppress the formation of a bread-loaf at the opening. Note that to afford complete fill in a re-entrant trench, the bread-loaf ratio needs to be ≤1; consequently, in addition to the requirement of a high superconformal step coverage, the effect of the inhibitor needs to be very strong. For growth of HfO_2 from 0.09 mTorr TDMA-Hf and 0.014 mTorr H_2O at 200 °C in the presence of a coflow of 0.063 mTorr H(acac), the observed inhibition effect in a re-entrant trench with an aspect ratio of 8 (defined as the depth divided by the average width) is not strong enough to keep the trench opening from pinching-off. As a result, a void is left inside the structure [Fig. 12(b)]. However, when the H(acac) pressure is increased to 0.09 mTorr, keeping other conditions unchanged, the void width significantly decreases and approaches a line seam.

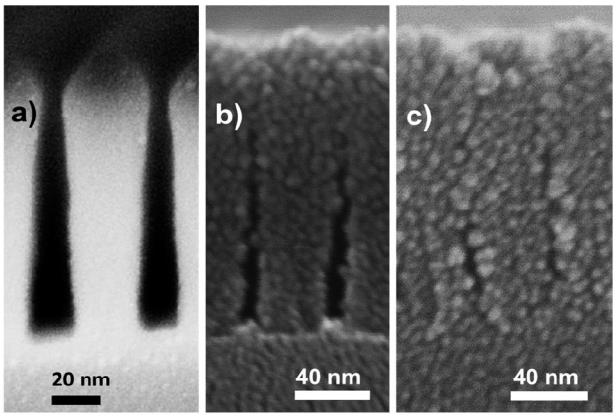

FIG. 12. SEM image of re-entrant shaped trenches of aspect ratio 8. (a) Before coating. (b) Coated using 0.09 mTorr TDMA-Hf, 0.014 mTorr H_2O, and 0.063 mTorr H(acac) at 200 °C for 20 min. (c) Coated using the same growth conditions as in (b) but with 0.09 mTorr of H(acac) for 45 min.

In view of the recognized difficulty associated with filling these re-entrant structures, we consider the coating profile obtained in Fig. 12(c) to be quite remarkable. Because saturation of the H(acac) inhibition effect occurs at higher pressure [Fig. 11(a)], higher H(acac) pressures would not further improve the result. The presence of a seam inside the trench in Fig. 12(c) may be a limitation of the underlying superconformal process itself, as opposed to a limitation of the inhibitor; enhancing the fraction of a forward-directed water flux would likely improve the filling.

E. Modeling the growth inhibitor effect

The microscopic surface reaction kinetics involving three reactants is inherently complex and cannot conclusively be determined from macroscopic film growth data. (We previously published a rate formalism for the case of two reactants, which is already complex.[23]) However, it is straightforward to show how a flux of inhibitor can modify the growth rates near the trench opening and thus prevent formation of a bread-loaf profile, while leaving the kinetics deeper in the trench relatively unchanged.

For the inhibitors that can eliminate the bread-loaf problem, H(hfac) and H(acac), the growth rate decreases with increasing inhibitor partial pressure (for the latter, above a certain threshold). This relationship allows us to propose a simple model in which the inhibitor has a constant sticking probability per wall collision; then, it is straightforward to calculate the rate at which the inhibitor sticks to the wall and thus decreases the film growth rate, as a function of depth in a trench. In this model, it is not necessary to know the intermediate microscopic steps such as the relationship between the surface coverage in inhibitor and the growth rate.

A ballistic transport-reaction model, fully described in Ref. 7, is used to calculate the net inhibitor flux distribution as a function of trench depth, which is then converted to a consumption rate by multiplying with the sticking probability, β (Fig. 13). Note that the β of interest here is the sticking probability in the presence of the other molecules in the growth reaction. For our purposes, we will assume that β is constant everywhere inside the trench; to be sure, real systems will fulfill this assumption only crudely, but the resulting conclusions should nevertheless illustrate general trends. We consider three different values of β (0.01, 0.1, and 0.9), referred to as low, medium, and high, respectively. A key relationship is that the film growth rate inside the

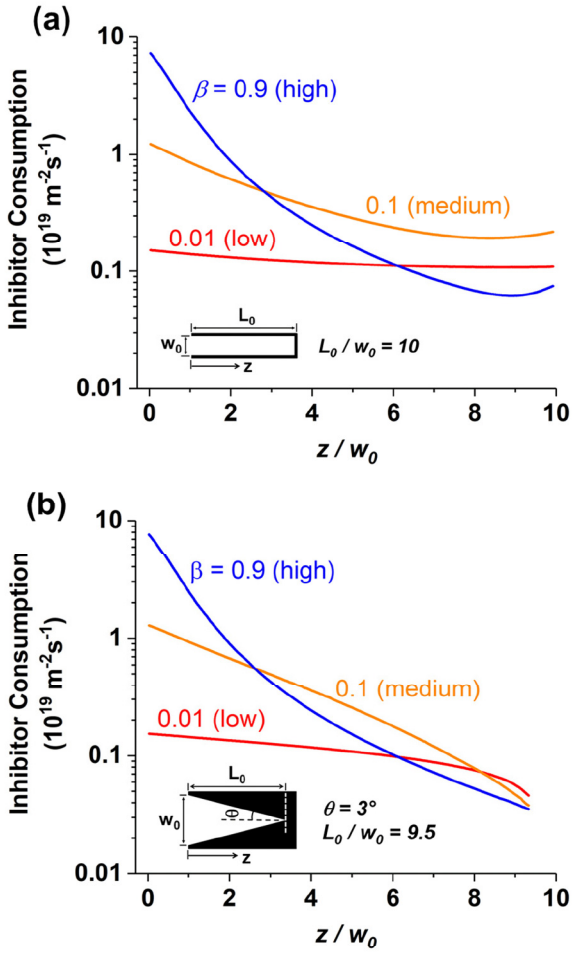

FIG. 13. Calculated H(acac) inhibitor consumption rate (in flux units) inside trenches as a function of normalized depth; three different sticking probability values, 0.01, 0.1, and 0.9, are considered. (a) Rectangular trench with an aspect ratio of 10. The slight upturn near to the bottom of the trench is due to molecules that arrive ballistically deep in the trench. Inset: Geometry of a rectangular trench showing the nominal aspect ratio (L_0/W_0). (b) V-shaped trench with sidewall tilt angle of 3° with respect to the trench axis. Ballistic transport still occurs but is less evident due to the vanishing width at the bottom of the V-shape. Inset: Geometry of a V-shaped trench; for $\theta = 3°$, the nominal aspect ratio (0.5/tan θ) is 9.5. The uniform H(acac) pressure outside the trench is 0.1 mTorr which is converted to an isotropic flux using the ideal gas law (Ref. 24).

trench will be reduced by the largest fraction at the depth at which the inhibitor consumption is maximum.

Let us first consider a trench with parallel sidewalls. For low β, the inhibitor consumption rate is nearly uniform at all depths in a rectangular trench with an aspect ratio 10 [Fig. 13(a)], whereas for a medium or high β, the inhibitor consumption drops with depth into the trench. (An exception is the small fraction of the isotropic flux from outside the trench that is oriented down the axis of the trench, impinges directly onto the bottom and is then redistributed on the sidewalls. If β is medium or high, this flux redistribution creates a minimum consumption point slightly above the bottom.) Thus, a maximum reduction in the bread-loaf effect, without adversely affecting growth rates at greater depths, will be found for "sticky" inhibitors having β values that are 0.1 or greater.

Let us next consider a V-shaped trench with a sidewall slope $\theta = 3°$, which we previously showed to be the minimum angle for superconformal growth of HfO_2, due to the maximum attainable ratio of forward-directed to isotropic water flux in our experimental setup. In such a V-shaped trench with $\theta = 3°$, the inhibitor consumption monotonically decreases with depth for all three (low, medium, or high) values of β; the minimum is at the bottom of the trench for any β [Fig. 13(b)]. This is because the solid angle between the trench opening and the sidewalls diminishes monotonically with depth. In a V-shaped trench, the larger drop in inhibitor consumption, relative to a rectangular trench, implies that the inhibitor has less effect on the growth rate deep in the feature, which helps to maintain the superconformal growth profile.

F. Crossover to uniform rate reduction

The results above show that, for the growth rate of HfO_2 films from 0.09 mTorr TDMA-Hf and 0.014 mTorr H_2O at 200 °C, increasing the pressure of the H(acac) inhibitor between 0.06 and 0.09 mTorr has an increasing beneficial effect on the bread-loaf effect, but that at 0.12 mTorr, the beneficial effect disappears. A similar crossover in behavior over a surprisingly small pressure range is also seen for H(hfac): at 0.27 Torr of the inhibitor, the bread-loaf near to the trench opening is eliminated without affecting the growth rate at greater depths, but at 0.32 mTorr, the growth rate is instead reduced everywhere within the trench.

We believe that this sudden change in behavior reflects a steep decrease in the inhibitor sticking probability at higher inhibitor pressure, owing to saturation of the surface coverage. The decrease in β enables more inhibitor to diffuse to greater depths, and as a result, rate reduction occurs everywhere, not just in the bread-loaf region. Thus, we must use these (or any other) inhibitors at a pressure that is large enough to reduce the growth rate near to the opening, but not so large that the inhibitor sticking probability falls and the inhibitor effect spreads deep into the structure.

Consistent with this view, the HfO_2 growth rates on planar substrates change very rapidly near these crossover pressures. For H(hfac) (Fig. 3), the film growth rate at 0.27 mTorr is ~20% of the rate with no inhibitor, but falls to ~10% at 0.32 mTorr. For H(acac) (Fig. 8), the growth rate falls from ~30% to ~10% when the inhibitor pressure is increased from 0.08 to 0.12 mTorr. It is reasonable to suppose that the decrease in the growth rate at the higher inhibitor pressures arises because the surface coverage of inhibitor reaches saturation, thus reducing the population of the rate-limiting species on the growth surface.

IV. CONCLUSION

We demonstrate that, for the superconformal growth of HfO_2 in trenches from TDMA-Hf and a forward-directed water flux, addition of small amounts of an isotropic coflow of a neutral inhibitor molecule can suppress bread-loaf formation at the trench opening without greatly affecting growth rates at greater depths. Consequently, the pinch-off of the trench opening is eliminated, and complete and seam-free fill

of HfO_2 is enabled. From coating experiments with different inhibitors, we found that both H(hfac) and H(acac) can enable complete fill in trenches with an aspect ratio of $\leq$10. Of these two molecules, H(acac) is the more desirable from a process perspective, because it is halogen-free. Both molecules lead to the incorporation of small amounts carbon into the film; for many device applications, a low level of carbon may be compatible with processing and property requirements.

We also demonstrate that the use of an inhibitor coupled with a superconformal film growth process based on forward-directed fluxes can potentially be used to fill re-entrant shaped trenches, provided that the growth process affords a sufficiently large superconformal step coverage.

Other inhibitor molecules, 3DMAS and MOTMS, are unable to suppress bread-loaf formation, but they increase the conformality of film growth in deep trenches in cases where complete filling is not required.

The inhibitor sticking rate on the trench sidewalls is modeled by simulating the inhibitor flux distribution using a Markov chain ballistic transport model; an inhibitor with a high reaction probability per wall collision is ideal to eliminate the pinch-off at the trench opening.

ACKNOWLEDGMENTS

The authors gratefully acknowledge support from SRC (Contract No. 2015-IN-2607); Sumeng Liu and Brian Trinh in the group of G.S.G. for precursor supply. G.S.G. acknowledges support from the National Science Foundation (NSF) (Grant No. CHE 16-65191). The authors also thank Bart van Schravendijk of Novellus Systems (now Lam Research Corporation) for supplying the SiN microtrench substrates as part of an earlier project. The *ex situ* materials characterization was carried out in the Center for Microanalysis of Materials at the Frederick Seitz Materials Research Laboratory, University of Illinois.

[1]F. Ayazi and K. Najafi, J. Microelectromech. Syst. **9**, 288 (2000).
[2]P. J. Ireland, Thin Solid Films **304**, 1 (1997).
[3]M. Nandakumar, A. Chatterjee, S. Sridhar, K. Joyner, M. Rodder, and I. C. Chen, *International Electron Devices Meeting 1998, Technical Digest (Cat. No. 98CH36217)*, San Francisco, CA, 6–9 December (IEEE, Piscataway, NJ, 1998), p. 133.
[4]E. Jordana *et al.*, *2007 4th IEEE International Conference on Group IV Photonics*, Tokyo, Japan, 19–21 September (IEEE, Piscataway, NJ, 2007), p. 222.
[5]A. Saynatjoki, T. Alasaarela, A. Khanna, L. Karvonen, P. Stenberg, M. Kuittinen, A. Tervonen, and S. Honkanen, Opt. Express **17**, 21066 (2009).
[6]*2015 International Technology Roadmap for Semiconductors* (Semiconductor Industry Association, Washington, DC, 2015).
[7]W. B. Wang and J. R. Abelson, J. Appl. Phys. **116**, 194508 (2014).
[8]T. K. Talukdar, W. B. Wang, G. S. Girolami, and J. R. Abelson, J. Vac. Sci. Technol. A **36**, 051513 (2018).
[9]T. K. Talukdar, S. Liu, Z. Zhang, F. Harwath, G. S. Girolami, and J. R. Abelson, J. Vac. Sci. Technol. A **36**, 051504 (2018).
[10]D. R. Cote, S. V. Nguyen, A. K. Stamper, D. S. Armbrust, D. Tobben, R. A. Conti, and G. Y. Lee, IBM J. Res. Dev. **43**, 5 (1999).
[11]A. K. Stamper, J. B. Lasky, and J. W. Adkisson, J. Vac. Sci. Technol. A **13**, 905 (1995).
[12]D. Cote, S. Nguyen, V. McGahay, C. Waskiewicz, S. Chang, A. Stamper, P. Weigand, N. Shoda, and T. Matsuda, *1996 1st International Symposium on Plasma Process-Induced Damage*, Santa Clara, California, 13–14 May (Northern California Chapter of the American Vacuum Society, Sunnyvale, CA, 1996), pp. 61–66.
[13]D. R. Cote, S. V. Nguyen, W. J. Cote, S. L. Pennington, A. K. Stamper, and D. V. Podlesnik, IBM J. Res. Dev. **39**, 437 (1995).
[14]S. Babar, N. Kumar, P. Zhang, and J. R. Abelson, Chem. Mater. **25**, 662 (2013).
[15]N. Kumar, A. Yanguas-Gil, S. R. Daly, G. S. Girolami, and J. R. Abelson, J. Am. Chem. Soc. **130**, 17660 (2008).
[16]S. Babar, E. Mohimi, B. Trinh, G. S. Girolami, and J. R. Abelson, ECS J. Solid State Sci. Technol. **4**, N60 (2015).
[17]Y. Yang "Chemical vapor deposition of metal diboride and metal oxide thin films from borohydride-bonded precursors," Ph.D. dissertation (University of Illinois at Urbana-Champaign, 2007), see http://hdl.handle.net/2142/82806.
[18]B. B. Burton, S. W. Kang, S. W. Rhee, and S. M. George, J. Phys. Chem. C **113**, 8249 (2009).
[19]E. Mohimi, Z. V. Zhang, S. Liu, J. L. Mallek, G. S. Girolami, and J. R. Abelson, J. Vac. Sci. Technol. A **36**, 041507 (2018).
[20]H. Sen Wei, C. C. Kuo, C. C. Jaing, Y. C. Chang, and C. C. Lee, J. Sol–Gel Sci. Technol. **71**, 168 (2014).
[21]R. C. Mehrotra, R. Bohra, and D. P. Gaur, *Metal B-diketonates and Allied Derivatives* (Academic, New York, 1978).
[22]A. Mameli, M. J. M. Merkx, B. Karasulu, F. Roozeboom, W. M. M. Kessels, and A. J. M. Mackus, ACS Nano **11**, 9303 (2017).
[23]A. Yanguas-Gil, N. Kumar, Y. Yang, and J. R. Abelson, J. Vac. Sci. Technol. A **27**, 1244 (2009).
[24]J. A. Venables, *Introduction to Surface and Thin Film Processes* (Cambridge University, Cambridge, 2000).
[25]See supplementary material at https://doi.org/10.1116/1.5068684 for more experimental results.